Simulation of a Rotating Chain with an Absolute Nodal Coordinate Formulation

Wan-Suk Yoo† · Oleg Dmitrochenko* · Dmitry Pogorelov**

절대절점좌표를 이용한 회전체인의 시뮬레이션

유완석† · Oleg Dmitrochenko* · Dmitry Pogorelov**

Key Words : Rotating chain(회전체인), Finite element method(유한요소법), Absolute nodal coordinate(절대절점좌표)

Abstract

A physically simple but mathematically cumbrous problem of rotating heavy chain with one fixed top point is studied. Nonlinear equation of its two-dimensional shapes of relative equilibrium is obtained and solved numerically. A linear case of small displacements is analyzed in terms of Bessel functions. The qualitative and quantitative behavior of the problem is discussed with the help of bifurcation diagram. Dynamics of the two-dimensional model near the equilibrium positions is studied with the help of simulation using the absolute nodal coordinate formulation (ANCF). The equilibriums are found instable, and the reason of instability is explained using a variational principle.

1. 서 론

The problem to be discussed here could probably have attracted many people's attention if they ever twirled a chain or rope in similar way that cowboys did. That is why it is surprisingly that this very interesting problem has almost been not described in the literature before. We only could find paper[1] and similar work of the same authors[2] that also stated that, to their knowledge, there has been no solutions of this *helicoseir* problem (from the Greek for *rotating rope*).

Our interest is to determine the exact shape of the helicoseir and the conditions under that they exist. The problem of determination of the shape of a continuous medium subjected to rotation and some force and constraint condition is, of course, not a new one and has its own history. For instance, the catenary problem[3]. The problems arising here often have a simple physical representation but surprisingly complicated equations. Such is the case of the helicoseir problem, which exact solution is unknown..

The studied phenomenon is a nonlinear mechanical system that is why we are especially interested in taking into account large displacements and choose the absolute nodal coordinate formulation[4] as the most proper in this case.

This paper is devoted to the two-dimensional simulation of the helicoseir problem. The variants of full nonlinear configuration equation are discussed in section 2, and the results are compared with these from the preceding paper[2]. The dynamical formulation and simulation results of 2D model using absolute nodal coordinate formulation are in section 3 and 4, respectively. Conclusions concerning instability of the model and the reasons are in sections 5.

2. Equations of a Helicoseeir in 2D Case

The object is a rotating inextensible rope or chain, which is fixed at the top point and twirled around a vertical axis under uniform gravitational field. Now we consider a two-dimensional problem, i.e. we assume that the shape of the helicoseir is a flat curve in plane xy, which is rotated around x axis,.

Let us consider the relative equilibrium of the part AB rotating around x axis. We should account inertia forces in addition to gravity forces, in accordance with d'Alembert principle. One of the equations of this quasi-

† 부산대학교 기계공학부
E-mail : wsyoo@pusan.ac.kr
TEL : (051)510-2328 FAX : (051)512-9835
* 부산대학교 CAE 연구실 Post doc researcher
** Brynsk State University, Brynsk, Russia

equilibrium is the momentum equation

$$\sum_{k\in AB} M_A(\mathbf{F}_k^{\text{active}}) + \sum_{k\in AB} M_A(\mathbf{F}_k^{\text{inert}}) = 0, \tag{1}$$

which states that total sum of moments M_A of gravity and inertia forces w.r.t. point A is zero.

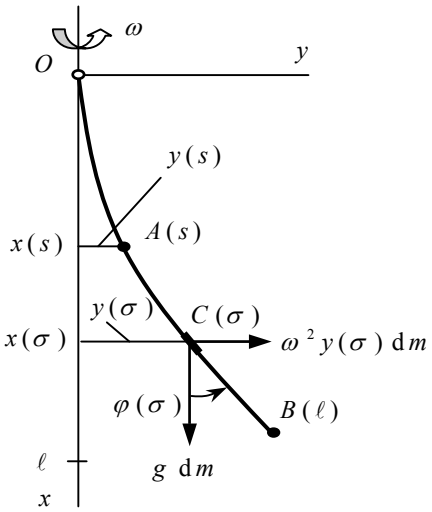

Fig. 1 A chain rotating along the vertical axis

The part AB begins at point A given by arc coordinate s with the origin in point O and end at point B when the arc coordinate is equal to the total length ℓ of the chain.

Consider an infinitesimal element $C(\sigma)$ of part AB marked by bold strip in. Let $x(\sigma)$ and $y(\sigma)$ be its Cartesian coordinates, where σ is an auxiliary arc coordinate running from s to length ℓ. These coordinates can be calculated as integrals

$$x(s) = \int_0^s \cos\varphi(\sigma)\,\mathrm{d}\sigma, \tag{2}$$

$$y(s) = \int_0^s \sin\varphi(\sigma)\,\mathrm{d}\sigma, \tag{3}$$

with an unknown function $\varphi(\sigma)$ of slope angle. This function defines the shape of our chain.

Using the introduced values, momentum equation (1) assumes the form

$$\int_s^\ell \omega^2 y(\sigma)\big(x(\sigma)-x(s)\big)\,\mu\,\mathrm{d}\sigma = \int_s^\ell g\,\big(y(\sigma)-y(s)\big)\,\mu\,\mathrm{d}\sigma \tag{4}$$

where μ is the linear density of the chain material.

In the latter equation, the values $x(s)$ and $y(s)$ can be taken out of integrals because the integration is assumed over σ:

$$g\,y(s)\int_s^\ell \mathrm{d}\sigma - \omega^2 x(s)\int_s^\ell y(\sigma)\,\mathrm{d}\sigma = \int_s^\ell y(\sigma)\big(g-\omega^2 x(\sigma)\big)\mathrm{d}\sigma.$$

To avoid integrals let us note that $\int_s^\ell \mathrm{d}\sigma = \ell - s$ and differentiate the latter equation with respect to s, applying a rule of derivating integrals with respect to their limits:

$$g\,(\ell-s)y'(s) - g\,y(s) - \omega^2 x'(s)\int_s^\ell y(\sigma)\,\mathrm{d}\sigma + \omega^2 x(s)y(s) = -y(s)\big(g-\omega^2 x(s)\big)$$

where we introduce the derivatives $x'(s) = \mathrm{d}x/\mathrm{d}s$ and $y'(s) = \mathrm{d}y/\mathrm{d}s$. Simplifying, the latter equation becomes

$$g(\ell-s)y'(s) - \omega^2 x'(s)\int_s^\ell y(\sigma)\,\mathrm{d}\sigma = 0. \tag{5}$$

Dividing by $g\,x'(s)$ we note that $y'(s)/x'(s) = \tan\varphi(s)$ (see definitions (2) and (3)) and introduce a new unknown function

$$t(s) = \tan\varphi(s) \tag{6}$$

as well as a new parameter

$$\alpha_\ell = \omega^2/g. \tag{7}$$

In paper [2], the authors used similar dimensionless frequency parameter $\alpha = \omega^2\ell/g$, so we can establish the following relationship between them:

$$\alpha_\ell = \alpha/\ell. \tag{8}$$

Then, after dividing by $g\,x'(s)$, equation (5) becomes

$$(\ell-s)\,t(s) - \alpha_\ell\int_s^\ell y(\sigma)\,\mathrm{d}\sigma = 0$$

and can be differentiated again:

$$(\ell - s)\, t' - t + \alpha_\ell y(s) = 0\,. \tag{9}$$

The final differentiation turns the equation into

$$(\ell - s)\, t'' - 2t' + \alpha_\ell \sin\varphi(s) = 0\,,$$

or, substituting sine in terms of tangent:

$$(\ell - s)\, t'' - 2t' + \frac{\alpha_\ell\, t}{\sqrt{1+t^2}} = 0\,. \tag{10}$$

Second-order differential equation (10) is the simplest known form of configuration equation describing the equilibrium shape of helicoseir. Using substitutions $\ell - s = \varsigma$, $t(s) = \tau(\varsigma)$ it can be shortened little again and represented in an equivalent form: $\varsigma\tau'' + 2\tau' + \alpha_\ell \tau\,(1+\tau^2)^{-1/2} = 0$ or even $(\varsigma^2\tau')' + \alpha_\ell \varsigma\tau(1+\tau^2)^{-1/2} = 0$, but it is more convenient for us to use argument s instead of ς.

3. Formulation and Simulation with ANCF

3.1 Absolute Nodal Coordinates

Since we do not know any analytical solution for dynamical and even for statical shapes of the helicoseir in nonlinear case, we try in this section to simulate its motion using a finite-element approach called absolute nodal coordinate formulation (ANCF).

The literature devoted to implementation of the ANCF for two-dimensional beams is numerous papers [5-15]. In our case of helicoseir, which is considered as a thin heavy beam, the most convenient abstraction is Euler-Bernoulli beam model.

The current implementation proposed below repeats most details published in paper[8]. However it has some special features. The first is that the helicoseir has no bending stiffness and only longitudinal forces appear. The second is the presence of centrifugal inertia forces due to rotation of the coordinate system.

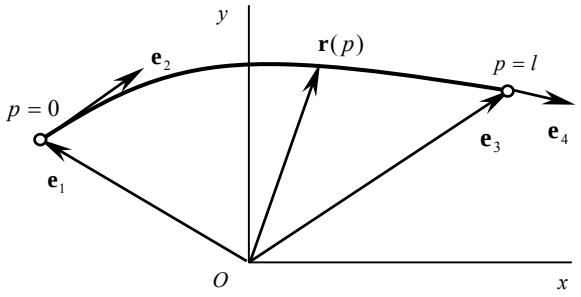

Fig. 2 Two-dimensional Euler-Bernoulli beam element using ANCF

A finite element of a 2D Euler-Bernoulli beam is shown in Fig. 2 . Its middle line is parameterized by value $p = 0 \ldots l$, where l is the initial length. Vector $\mathbf{e}$ of its absolute nodal coordinates contains position vectors $\mathbf{e}_1$, $\mathbf{e}_3$ of the end points and tangent slope vectors $\mathbf{e}_2$, $\mathbf{e}_4$ at these points:

$$\mathbf{e} = \{\mathbf{e}_1^{\mathrm{T}}, \mathbf{e}_2^{\mathrm{T}}, \mathbf{e}_3^{\mathrm{T}}, \mathbf{e}_4^{\mathrm{T}}\}^{\mathrm{T}}\,. \tag{11}$$

Note that the components of vectors $\mathbf{e}_k$ are not supposed small and tangent vectors $\mathbf{e}_2$, $\mathbf{e}_4$ may have non-unit length.

The position of an arbitrary point of the element centerline can be found as

$$\mathbf{r} = \sum_{k=1}^{4} s_k \mathbf{e}_k\,, \tag{12}$$

where the beam shape functions are introduced:

$$\begin{aligned} s_1(p) &= 1 - 3\xi^2 + 2\xi^3, \quad s_2(p) = l(\xi - 2\xi^2 + \xi^3), \\ s_3(p) &= 3\xi^2 - 2\xi^3, \qquad s_4(p) = l(\xi^3 - \xi^2), \end{aligned} \qquad \xi = p/l.$$

3.2 EOM and Mass matrix

Equations of motion of the beam element can be obtained from Lagrange equations

$$\frac{\mathrm{d}}{\mathrm{d}t}\left(\frac{\partial T}{\partial \dot{\mathbf{e}}}\right) - \frac{\partial T}{\partial \mathbf{e}} + \frac{\partial U}{\partial \mathbf{e}} = \frac{\delta W}{\delta \mathbf{e}}$$

with the kinetic energy $T = \frac{1}{2}\int_0^l \mu \dot{\mathbf{r}}^{\mathrm{T}} \dot{\mathbf{r}}\, \mathrm{d}p$ (μ is the linear density in *kg*/*m*), the strain energy U and the virtual work δW of external gravity and centrifugal forces, see below.

Taking into account relation (12), we find that the equations assume the matrix form[8]

$$\mathbf{M}\,\ddot{\mathbf{e}} + \mathbf{Q}^{\mathrm{e}}(\mathbf{e}) = \mathbf{Q}^{\mathrm{gr}} + \mathbf{Q}^{\mathrm{cf}}(\mathbf{e})\,, \tag{13}$$

where

$$\mathbf{M} = \frac{\mu l}{420}\begin{bmatrix} 156\mathbf{I} & & & \text{symm.} \\ 22l\mathbf{I} & 4l^2\mathbf{I} & & \\ 54\mathbf{I} & 13l\mathbf{I} & 156\mathbf{I} & \\ -13l\mathbf{I} & -3l^2\mathbf{I} & -22l\mathbf{I} & 4l^2\mathbf{I} \end{bmatrix}.$$

$$\mathbf{M}_{ij} = \underbrace{\mu \int_0^l s_i s_j\, \mathrm{d}p}_{M_{ij}}\, \mathbf{I} = M_{ij}\mathbf{I}$$

is the mass matrix represented in a block form, $\mathbf{I} = \mathbf{diag}(1,1)$ is identity matrix. The generalized gravity

$\mathbf{Q}^{\mathrm{gr}}$ and centrifugal inertia forces $\mathbf{Q}^{\mathrm{cf}}$ due to rotation of the non-inertial reference frame are introduced in section 3.3, while the generalized elastic forces are briefly reviewed in section 3.4.

3.3 Generalized Forces

Consider a 2D beam finite element in the coordinate frame *xy*, which is rotating around axis *x* as shown in Fig. 3. This fact results in the explicit arising of centrifugal inertia forces applied to the FE, which have not been published in the literature before. That is why we start with the thorough introducing more usual generalized gravity forces and after that turn to the inertia forces.

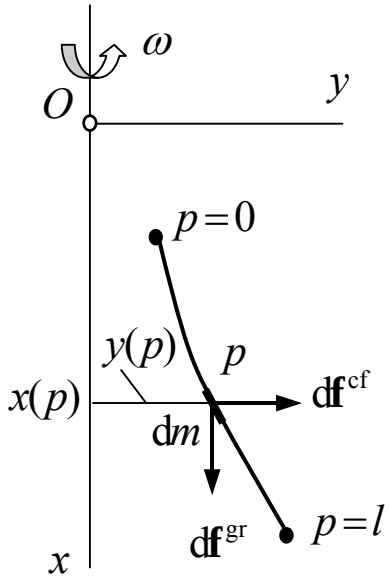

Fig. 3 Gravity and centrifugal forces applied to a FE

Gravity force applied to an infinitesimal particle with mass dm is $\mathrm{d}\mathbf{f}^{\mathrm{gr}} = \mathrm{d}m\, g\, \mathbf{i} = \mu g\, \mathrm{d}p\, \mathbf{i}$, where d$p$ is length of the particle and $\mathbf{i} = \{1, 0\}^{\mathrm{T}}$ is the unit vector of axis *Ox*. Then we calculate the virtual work of this gravity force and intergrate it over the beam FE:

$$\delta W^{\mathrm{gr}} = \int_{\mathrm{FE}} \delta \mathbf{r}^{\mathrm{T}}\, \mathrm{d}\mathbf{f}^{\mathrm{gr}} = \int_0^l \left(\sum_{i=1}^4 \delta \mathbf{e}_i^{\mathrm{T}} s_i \right) \mu g\, \mathrm{d}p\, \mathbf{i} = \sum_{i=1}^4 \delta \mathbf{e}_i^{\mathrm{T}} \vec{s}_i\, \mu g\, \mathbf{i}.$$

Here we use relation (12) as well as notation $\vec{s}_i = \int_0^l s_i(p)\, \mathrm{d}p$ for the integration of shape functions s_i.

Now, the generalized forces are calculated as gradients: $\mathbf{Q}_i^{\mathrm{gr}} = \delta W^{\mathrm{gr}} / \delta \mathbf{e}_i = \vec{s}_i \mu g\, \mathbf{i}$, and full vector corresponding to gravity forces is

$$\mathbf{Q}^{\mathrm{gr}} = \begin{Bmatrix} \mathbf{Q}_1^{\mathrm{gr}} \\ \mathbf{Q}_2^{\mathrm{gr}} \\ \mathbf{Q}_3^{\mathrm{gr}} \\ \mathbf{Q}_4^{\mathrm{gr}} \end{Bmatrix} = \begin{Bmatrix} (\mu g l/2)\, \mathbf{i} \\ (\mu g l^2/12)\, \mathbf{i} \\ (\mu g l/2)\, \mathbf{i} \\ -(\mu g l^2/12)\, \mathbf{i} \end{Bmatrix}.$$

Similar calculations can be done for the elementary centrifugal force

$$\mathrm{d}\mathbf{f}^{\mathrm{cf}} = \mathrm{d}m\, \omega^2 y\, \mathbf{j} = \mu \omega^2 y\, \mathrm{d}p\, \mathbf{j},$$

where $\mathbf{j} = \{0, 1\}^{\mathrm{T}}$ is the unit vector of axis *Oy*. The component y is the 2nd component of the radius-vector $\mathbf{r}$ of the beam particle and can be calculated as [8]

$$y = (\mathbf{r})_2 = \sum_{k=1}^4 s_k (\mathbf{e}_k)_2, \qquad (14)$$

where $(\mathbf{e}_k)_2$ denotes the 2nd component of the vector $\mathbf{e}_k$. The latter vectors are parts of vector of nodal coordinates (11). If $\mathbf{e}$ is treated as a vector containing scalar values then $\mathbf{e} = \{e_1, e_2, \ldots, e_8\}^{\mathrm{T}}$. It is evidently then that $(\mathbf{e}_k)_2 = e_{2k}$ in formula (14).

Virtual work of inertia forces takes the form

$$\delta W^{\mathrm{cf}} = \int_{\mathrm{FE}} \delta \mathbf{r}^{\mathrm{T}}\, \mathrm{d}\mathbf{f}^{\mathrm{cf}} = \int_0^l \left(\sum_{i=1}^4 \delta \mathbf{e}_i^{\mathrm{T}} s_i \right) \mu \omega^2 \sum_{k=1}^4 s_k e_{2k}\, \mathrm{d}p\, \mathbf{j}, = \sum_{i=1}^4 \delta \mathbf{e}_i^{\mathrm{T}} \omega^2 \sum_{k=1}^4 M_{ik} e_{2k}\, \mathbf{j}$$

where M_{ik} are scalar components of mass matrix, and generalized forces are

$$\mathbf{Q}_i^{\mathrm{cf}} = \frac{\delta W^{\mathrm{cf}}}{\delta \mathbf{e}_i} = \omega^2 \sum_{k=1}^4 M_{ik} e_{2k} \mathbf{j}.$$

The full vector of generalized centrifugal forces is calculated by formula

$$\mathbf{Q}^{\mathrm{cf}}(\mathbf{e}) = \omega^2\, \mathbf{M} \begin{Bmatrix} e_2 \mathbf{j} \\ e_4 \mathbf{j} \\ e_6 \mathbf{j} \\ e_8 \mathbf{j} \end{Bmatrix},$$

using the definition of the mass matrix.

3.4 Strain energy

The vector of generalized elastic forces $\mathbf{Q}^{\mathrm{e}} = \partial U / \partial \mathbf{e}$ is the most cumbrous one due to complexity of the strain energy U. We assume the helicoseir to be a chain (without bending stiffness) that is why its energy is that of longitudinal deformation only:

$$U = \frac{1}{2}\int_0^l EA\varepsilon^2 \,\mathrm{d}p$$

with the longitudinal deformation ε. Longitudinal stiffness EA is supposed constant within the beam element.

Longitudinal elastic forces are gradient vectors of the corresponding strain energy U:

$$\mathbf{Q}_i^{\mathrm{e}} = \frac{\partial U}{\partial \mathbf{e}_i} = EA\int_0^l \varepsilon \frac{\partial \varepsilon}{\partial \mathbf{e}_i}\mathrm{d}p \,. \qquad (15)$$

This expression contains the longitudinal deformation

$$\varepsilon = \left\|\mathbf{r}'\right\| - 1 = \sqrt{\mathbf{r}'^{\mathrm{T}}\mathbf{r}'} - 1 \approx \frac{1}{2}(\mathbf{r}'^{\mathrm{T}}\mathbf{r}' - 1)\,, \qquad (16)$$

where prime denotes derivative w.r.t. arc parameter p. In paper [8], it was shown that the latter formula represents Green's non-linear strain-displacement relationships[16] in the 1-dimentional case.

The longitudinal deformation (16) and its gradients can be expressed in terms of shape functions and nodal coordinates (12) as follows:

$$\varepsilon = \frac{1}{2}\left(\sum_{m=1}^{4}\sum_{n=1}^{4} s'_m s'_n \mathbf{e}_m^{\mathrm{T}}\mathbf{e}_n - 1\right), \qquad (17)$$

$$\frac{\partial \varepsilon}{\partial \mathbf{e}_i} = \sum_{k=1}^{4} s'_i s'_k \mathbf{e}_k \,. \qquad (18)$$

Direct substitution of expressions (17) and (18) into (15) leads to elastic forces and the Jacobian matrix of elastic forces were explained in paper[8].

4. Simulation Results

Due to absence of analytical solution for dynamical shapes of the helicoseir, we used absolute nodal coordinate formulation implemented in the program package Universal Mechanism(www.umlab.ru) for numerical dynamic analysis of the model.

We used the following parameters of the helicoseir: length $\ell = 1$ m, gravity acceleration $g = 9.81$ m/s^2, angular velocity of rotation: $\omega = 12$ rad/s ($\alpha = 14.7$) for the second form and $\omega = 20$ rad/s ($\alpha = 40.8$) for the third form.

We used a high value of Young modulus $E = 10^{10}$ Pa in finite-element models in order to approximate an inextensible chain assumed in theoretical investigations in section 2. Density μ and geometrical parameters of the cross section are not significant and can take arbitrary values.

Damping forces were simulated using simple Rayleigh model[16].

$$\mathbf{Q}^{\mathrm{damp}} = \gamma\, \mathbf{M}\, \dot{\mathbf{e}}\,,$$

where $\mathbf{M}$ is the mass matrix, γ is the damping ratio, which numerical value was set to 10 to provide high dissipation of energy.

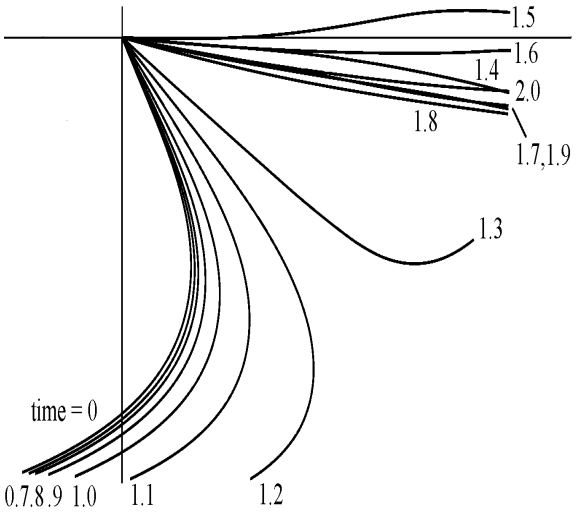

Fig. 4 Instability of the 2nd mode in 2D ($\omega = 12$ rad/s, $\alpha = 14.7$)

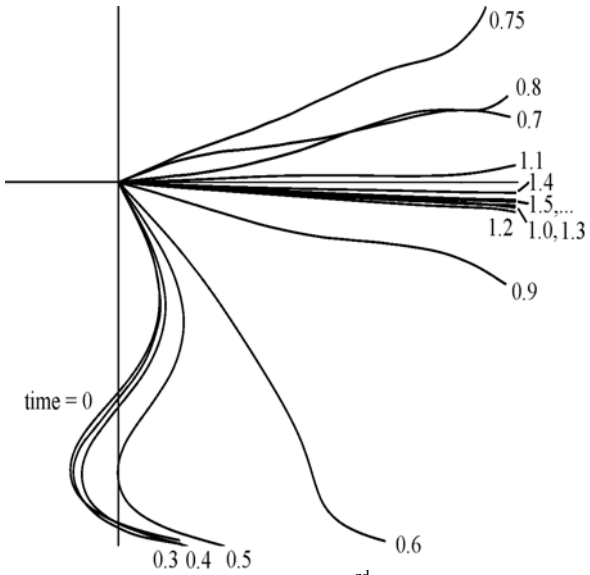

Fig. 5 Instability of the 3rd mode in 2D ($\omega = 20$ rad/s, $\alpha = 40.8$)

Initial configurations of the helicoseir were calculated numerically as described in section 2. Initial velocities were set to 0. The sequential positions of the helicoseir during its motion are represented in Fig. 4 and Fig. 5. The figures show instability of both 2nd and 3rd modes: because the initial positions obtained from numerical approximate solution are not exact equilibrium positions, the helicoseir runs quickly away from these to a position corresponding to the 1st mode at given frequency parameter α. Thus, it can be shown that the numerical simulation proves instability of all higher equilibrium modes except the 1st one.

5. 결 론

We considered a helicoseir problem, which is phenomenologically easy-to-implement but represented by surprisingly complicated nonlinear equations of relative equilibrium. We studied the preceding paper by Silverman at al., redeveloped and simplified their equations in two-dimensional case as well as the boundary conditions. This allowed us to obtain the bifurcation diagram of this problem.

We also studied the stability of the equilibrium configurations of the two-dimensional model with the help of simulation using the absolute nodal coordinate formulation; we found that all higher modes of the equilibrium except the first one are instable. This means that the helicoseir in reality has no relative equilibrium positions and its shape is three-dimensional; its motion, probably, looks like self-excited oscillations.

In the future, we intend to study full three-dimensional model of the helicoseir.

Acknowledgements

The authors thank the Ministry of Science and Technology of Korea for its financial support (grant (M1-0203-00-0017) under the National Research Laboratory project. The research was also supported by RFBR (02-01-00364-A) and by the scientific program “Universities of Russia” (UR.04.01.046).

참고문헌

(1) Silverman, M. P., Strange, Wayne, Lipscombe, T. C., ‘‘String theory’: equilibrium configurations of a helicoseir’, in European Journal of Physics 19, 379-387, 1998.

(2) Silverman, M. P., Strange, W., Lipscombe, T. C., ‘The shapes of a twirled keychain’, in Proc. of American Physical Society and American Association of Physics Teachers, Columbus, OH, 18-21 April 1998.

(3) Weinstock, R. Calculus of variations, Dover, New York, 1974.

(4) Shabana, A. A., ‘Flexible Multibody Dynamics: Review of Past and Recent Developments’, in Multibody System Dynamics 1, 1997, 189-222.

(5) Berzeri, M. and Shabana, A. A., ‘Development of Simple Models for the Elastic Forces in the Absolute Nodal Co-ordinate Formulation’, in Journal of Sound and Vibration 235(4), 2000, 539-565.

(6) Omar, M. A. and Shabana, A. A., ‘A Two-Dimensional Shear Deformation Beam for Large Rotation and Deformation’, in Journal of Sound and Vibration 243(3), 2001, 565-576.

(7) Takahashi, Y., and Shimizu, N. ‘Study on Elastic Forces of the Absolute Nodal Coordinate Formulation for Deformable Beams’, in ASME Proceedings of Design Engineering Technical Conference, VIB-8203, Las Vegas, 1999.

(8) Yoo W.-S., Lee J.-H., Park S.-J., Sohn J.-H., Dmitrochenko O.N., Pogorelov D.Yu., ‘Large Oscillations of a Thin Cantilever Beam: Physical Experiments and Simulation using Absolute Nodal Coordinate Formulation’, in Nonlinear Dynamics Journal, Vol. 34, Issue 1, Oct 2003, 2003, 3-29.

(9) Dmitrotchenko, O. N., ‘Efficient Simulation of Rigid-Flexible Multibody Dynamics: Some Implementations and Results’, in Proc. of NATO ASI on Virtual Nonlinear Multibody Systems 1, W. Schielen and M. Valášek (Eds.), Prague, 2002, 51-56.

(10) Mikkola, A. M. and Shabana, A. A., ‘A New Plate Element based on the Absolute Nodal Coordinate Formulation’, in Proc. of ASME 2001 DETC, Pittsburgh, 2001.1.

(11) Omar, M. A. and Shabana, A. A., ‘A Two-Dimensional Shear Deformation Beam for Large Rotation and Deformation’, in Journal of Sound and Vibration 243(3), 2001, 565-576.

(12) Pogorelov, D., ‘Some developments in computational techniques in modeling advanced mechanical systems’, in Proceedings of IUTAM Symposium on Interaction between Dynamics and Control in Advanced Mechanical Systems, D. H. van Campen (Ed.), Kluwer Academic Publishers, Dordrecht, 1997, 313-320.

(13) Pogorelov, D., ‘Differential-algebraic equations in multibody system modeling’, in Numerical Algorithms 19, Baltzer Science Publishers, 1998, 183-194.

(14) Schwertassek, R., ‘Flexible Bodies in Multibody Systems’, in Computational Methods in Mechanical Systems 161, Springer Verlag, 1997, 329-363.

(15) Shabana, A. A. and Yakoub, R. Y., ‘Three Dimensional Absolute Nodal Coordinate Formulation for Beam Elements: Theory’, in Journal of Mechanical Design 123, 2001, 606-621.

(16) Zienkiewicz, O. C. and Taylor, R. L., The Finite Element Method, 4th Edition, Volume 2: Solid and Fluid Mechanics, McGraw-Hill Book Company, 1991.